MATHEMATICAL MODEL AND SIMULATION OF A PNEUMATIC APPARATUS FOR IN-DRILLING ALIGNMENT OF AN INERTIAL NAVIGATION UNIT DURING HORIZONTAL WELL DRILLING

Alexander Djurkov, Justin Cloutier, Martin P. Mintchev

Abstract: Conventional methods in horizontal drilling processes incorporate magnetic surveying techniques for determining the position and orientation of the bottom-hole assembly (BHA). Such means result in an increased weight of the drilling assembly, higher cost due to the use of non-magnetic collars necessary for the shielding of the magnetometers, and significant errors in the position of the drilling bit. A fiber-optic gyroscope (FOG) based inertial navigation system (INS) has been proposed as an alternative to magnetometer -based downhole surveying. The utilizing of a tactical-grade FOG based surveying system in the harsh downhole environment has been shown to be theoretically feasible, yielding a significant BHA position error reduction (less than 100m over a 2-h experiment). To limit the growing errors of the INS, an in-drilling alignment (IDA) method for the INS has been proposed. This article aims at describing a simple, pneumatics-based design of the IDA apparatus and its implementation downhole. A mathematical model of the setup is developed and tested with Bloodshed Dev-C++. The simulations demonstrate a simple, low cost and feasible IDA apparatus.

Keywords: Mathematical Modeling, Measurement-While-Drilling, In-Drilling Alignment

ACM Keywords: Mathematical Modeling

List of Abbreviations

BHA	Bottom-hole assembly	INS	Inertial Navigation System
FOG	Fiber-optic gyroscope	MWD	Measuring-while-drilling
IDA	In-drilling alignment	ZUPT	Zero velocity update
IMU	Inertial Measurement Unit		

Nomenclature:

a	Orifice area (m^2)	Pa	Air Pressure in Chamber A
Aa	Piston area enclosing Chamber A (m^2)	P_b	Air Pressure in Chamber B
Ab	Piston area enclosing Chamber B (m^2)	R	Gas constant for air (287 J/kg/K)
c_p	Constant air pressure specific heat (1003.5 $Jkg^{-1}K^{-1}$)	$T_{a,\,b}$	Cylinder's chamber temperatures (K)
c_q	Orifice Discharge Coefficient	$T_{s,\,ex}$	Air tank temperatures (K)
c_v	Constant air volume specific heat (718.6$Jkg^{-1}K^{-1}$)	V_{da}	Chamber A dead volume (m^3)
m_a	Mass of air in Chamber A (kg)	V_{db}	Chamber B dead volume (m^3)
m_b	Mass of air in Chamber B (kg)	x	Displacement of piston
M	Combined mass of piston, piston rod and IMU (kg)	x_1	Cylinder's stroke

1. Introduction

1.1 Conventional Horizontal Drilling Techniques

Horizontal drilling features several advantages when it comes to oil exploration and production. First, it facilitates the accessibility of reservoirs in complex locations: under riverbeds, mountains and even cities [1]. Secondly, if a particular reservoir is characterized by a large surface area, but is distributed over a thin horizontal layer, a horizontal well will yield a larger contact area with the reservoir and thus lead to a higher productivity and longevity when compared to vertical ones [2]. Present applications of horizontal wells include intersecting of fractures; eliminating of coning problems in wells with gas and water coning problems; the improving of draining area per well in gas production, resulting in a reduction of the number of wells required to drain the reservoir; and providing larger reservoir contact area and enhancing injectivity of an injection well [3].

The drilling of a directional (horizontal) well begins by drilling vertically from the surface to a kick-off point at a predetermined depth. Then, the well bore is deviated intentionally from the vertical at a controlled rate. To

implement this complex drilling trajectory, measurement-while-drilling (MWD) equipment, steerable setup and surveying sensors must be incorporated within the drilling assembly [4]. The drilling assembly utilizes a diamond bit and a mud turbo-drill motor installed in front of a trajectory control sub, nonmagnetic drill collars which include the magnetic surveying sensors, and a drill pipe [5], (Fig.1).

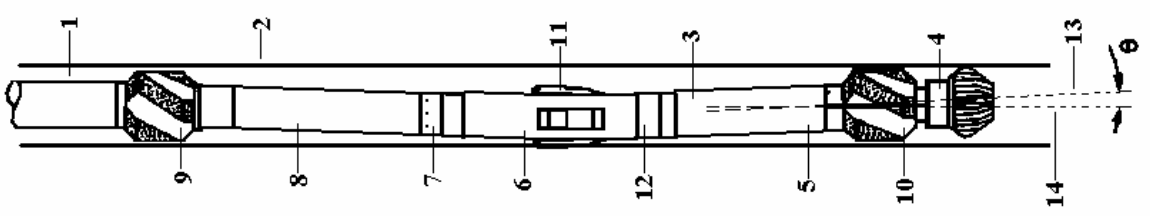

Fig.1: Drilling Assembly: 1 – drill string, 2 – borehole, 3 – bottom hole assembly (BHA), 4 – drill bit, 5 – drilling motor, 6 – trajectory control sub, 7 – bypass sub, 8 – MWD tool included in nonmagnetic collars, 9, 10 – upper and lower stabilizers for centering the drilling assembly in the borehole, 11 – stabilizer blades, 12 – induced bend to provide angular offset (θ) between the axis of the drill bit (13) and the center line (14).

1.2 Principles of Magnetic Surveying

The conventional measurement-while-drilling (MWD) surveying system presently utilizes three-axis accelerometers and three-axis magnetometers fixed in three mutually orthogonal directions [13]. At a certain predetermined surveying stations, the drilling assembly is brought to rest. At that point, the body frame of the MWD surveying system, formed by the axes of the accelerometers and magnetometers, is an angular transformation of the reference (North-East-Vertical) frame. Since the position of the bottom-hole assembly (BHA) is known, the direction and magnitude of Earth's acceleration are known as well. By comparing the acceleration vector formed from the measurements of the three accelerometers with the known vector of Earth's gravitational acceleration in the reference frame, the pitch (θ) and row (Φ) can be calculated (Fig.2) [7].

Then, the measurements from the magnetometers are combined with the calculated pitch and row to determine the azimuth angle (Ψ). The BHA trajectory is then computed by assuming a certain trajectory between the two successive stations.

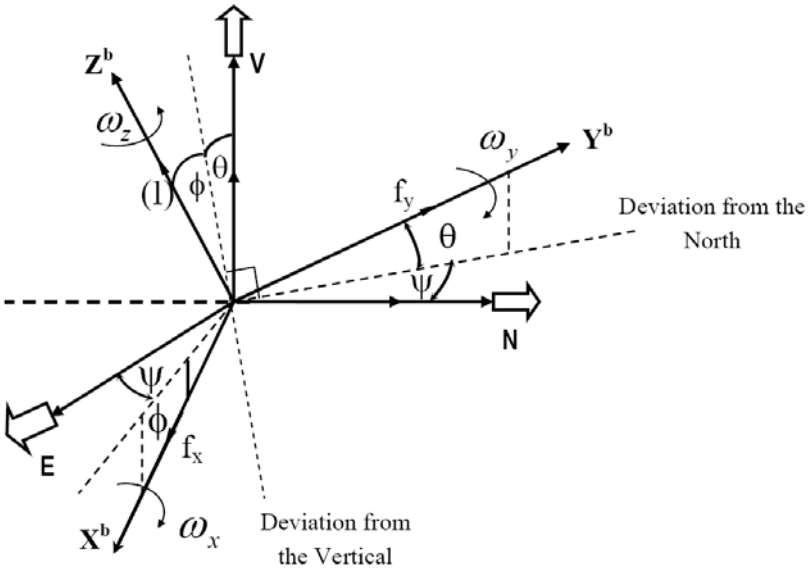

Fig.2: Orientation of the MWD magneto-surveying system with respect to North, East, and Vertical directions: the pitch (θ), the roll (Φ), and the azimuth (Ψ). In the drawing, X^b, Y^b and Z^b form the body frame, with its axes coinciding with the axes of the accelerometers and magnetometers. E, N, and V denote East, North, and Vertical and form the reference frame. The measured accelerations along the axes x, y and z of the body frame are respectively f_x, f_y, and f_z. The measured angular rates in the body frame about the x, y and z axes are respectively ω_x, ω_y, and ω_z.

1.3 Problems with MWD Magneto-Surveying System

Several external factors affect the performance of the magnetic surveying sensors. Such factors encompass the presence of randomly located ore deposits and geomagnetic influences. Moreover, the dynamic behavior of the magnetometers is negatively affected by magnetic interferences from the drill string. This requires the utilization of nonmagnetic collars for protecting the magnetic sensors. Although the accuracy of the magneto-surveying system increases with length of the nonmagnetic collars, this results in heavier and more costly MWD apparatus. Additionally, another source of error is introduced. Since the surveying sensors are located approximately 20 meters away from the drill bit, some rotations of the near-drill bit assembly may not be recognized [6].

1.4 Review of Current Inertial Navigation System (INS) -Based Navigation

In order to avoid the problems associated with magnetometers and non-magnetic collars, an INS based inertial measurement unit (IMU) incorporating a single fiber-optic gyroscope (FOG) and three-axis accelerometer has been proposed [7]. The INS determines the position, velocity and orientation of the drilling assembly in three-dimensional space by integrating the measured components of the acceleration (provided by the accelerometers) and the angular velocity (provided by the gyroscope). However, due to the small errors in the measurements of the accelerometers and the fiber-optic gyroscope, a continuous error growth in the position and the velocity of the BHA is observed [8]. Several approaches to limit this error growth have been proposed.

The first approach is based on continuous surveying with the aid of velocity and altitude updates through a Kalman filter. It has been reported that this method yields an inclination and azimuth angle errors of less than 0.4º and 1º, respectively, over a two-hour experiment. Moreover, the altitude errors have not exceeded ±0.5m over the entire experiment, while the errors along the East and North directions, dependant on the accelerometer bias, have been kept less than 50m and 20m respectively, over a two hour experiment [8].

The second approach was applied when velocity updates were not available. The approach involved the interrupting of the BHA motion at some predetermined station to apply the velocity zero update (ZUPT) for resetting the velocity errors and stopping the growth of position errors. The ZUPT approach was associated with position errors of less than 25m and 100m along the East and North directions respectively [8]. However, these results did not show substantial advantage over standard magnetic surveying.

A third method, called the In-Drilling Alignment Method (IDA), involves the induction of motion on the IMU in the horizontal North-East plane, while the entire bottom-hole assembly (BHA) is at rest. If the acceleration of the IMU at any time during the induced motion is known more precisely than the accuracy of the accelerometers on the IMU, the observations may be used as acceleration updates to align the accelerometers. Separately, an angular motion of the IMU about the axis of its gyroscope may be induced with accurately known angular rate and be used as an update for the gyroscope [9]. Such an IDA apparatus that will perform effectively in bore-hole drilling conditions has not been designed.

The aims of this paper are: (1) to design an In-Drilling Alignment apparatus for testing this newly-proposed concept; and (2) to mathematically model the expected results provided by such an apparatus.

2. Methods and Materials

2.1 Inducing Motion on the IMU in the North-East Horizontal Plane

A pneumatically-based solution is proposed for inducing a motion on the IMU in the North-East horizontal plane while the BHA is at rest. A compact, cylindrical capsule containing an IMU, RF transmitter and a small battery to power the IMU and the transmitter is attached to the end of a piston rod of a pneumatic cylinder via a bearing. The bearing allows the capsule to rotate freely around the cylinder's rod. By correctly regulating the pressure on each side of the piston, desired linear accelerations of the piston rod-IMU assembly can be obtained (Fig.3).

Fig.3: In-Drilling Alignment Apparatus

This linear motion can further be employed for inducing an angular motion on the IMU about the axis of one its gyroscopes. On the exterior surface of the cylindrical capsule, around its axis, ball bearings are positioned in a helical pattern. Similar helical thread is machined on the inner side of a pipe, to allow the bearings on the capsule to smoothly traverse along it. Thus, any linear motion induced on the capsule by the pneumatic cylinder will simultaneously cause an angular motion. If the linear acceleration of the IMU-containing capsule and the angular step of the helical thread are accurately known, then the angular acceleration of the capsule can be calculated easily. This in turn can be integrated to yield the angular rotation rate of the capsule (Fig.4).

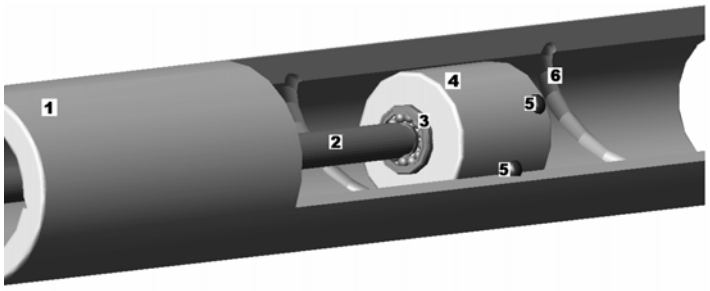

Fig.4: Schematic of the angular motion inducing mechanism: 1-pipe, 2-pneumatic cylinder rod, 3-bearing, 4-capsule enclosing IMU, battery and RF transmitter, 5-ball bearings aligned in a helical pattern over the surface of the capsule, 6-helical thread machined on the interior surface of the pipe.

2.2 Monitoring the Induced Motion of the IMU

The principle of the magnetostrictive effect is employed for monitoring the position of the piston in the pneumatic cylinder. For this purpose, the piston is equipped with tiny magnets, and a special piston position-sensing unit is installed along the cylinder (Fig.5) [11].

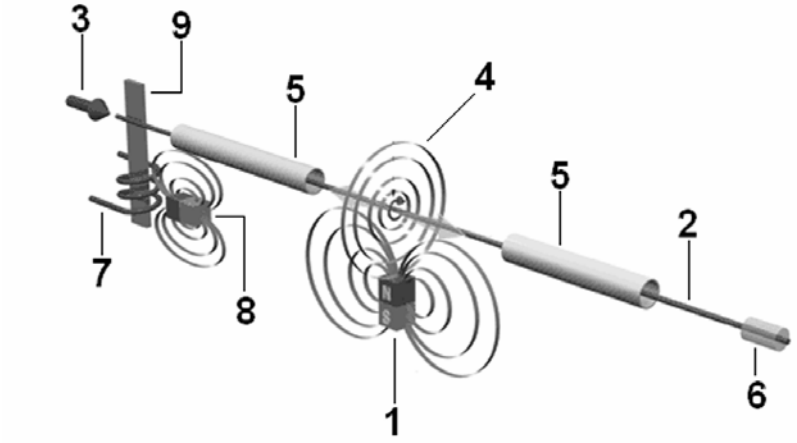

Fig. 5: Schematic of the operation of a magnetostrictive effect-based piston position sensing unit: 1-piston magnet, 2-waveguide, 3-short current pulse, 4-magnetic field around the waveguide due to the current pulse (3), 5-protective casing, 6-dampener, 7-mechanical wave detecting coil, 8-magnet providing a magnetic field in which the detecting coil is located (7), 9-strip along which the deformation wave is transmitted to the coil.

The unit consists of a “waveguide” made of a special nickel-alloy tube through which runs a copper wire. The initiation of a measurement is denoted by a short electric pulse through this wire, which sets up a circular magnetic field around it. At the point along the “waveguide” where the produced field intersects the perpendicular magnetic filed due to the magnets located in the piston of a pneumatic cylinder, an elastic deformation of the nickel-alloy tube is caused according to the magnetostrictive effect. The component of the deformation wave that traverses the “waveguide” toward its back end is dampened, while the component that arrives at the signal converter is transformed into an electric pulse. Since the travel time for the pulse is directly proportional to the

position of the magnetic piston [11], by determining the elapsed time between the initiating pulse and received pulse, the piston's position can be estimated with high accuracy in the order of 5μm [11].

Once the position of the piston is accurately known, a differentiation yields its velocity and acceleration. However, since the IMU capsule is affixed to the piston rod of the pneumatic cylinder, its linear component of motion is completely defined. Moreover, the angular rate of the IMU around the axis of the pneumatic cylinder can be calculated according to:

$$\omega = \boldsymbol{v} \cdot \lambda \tag{1}$$

where (ω) is the angular speed, (v) is the linear speed and (λ) is the angular step of the machined helical thread.

2.3 Pneumatic Setup of the IDA Apparatus

The following simplified pneumatic setup is proposed for inducing and controlling the motion of the IMU (Fig.6).

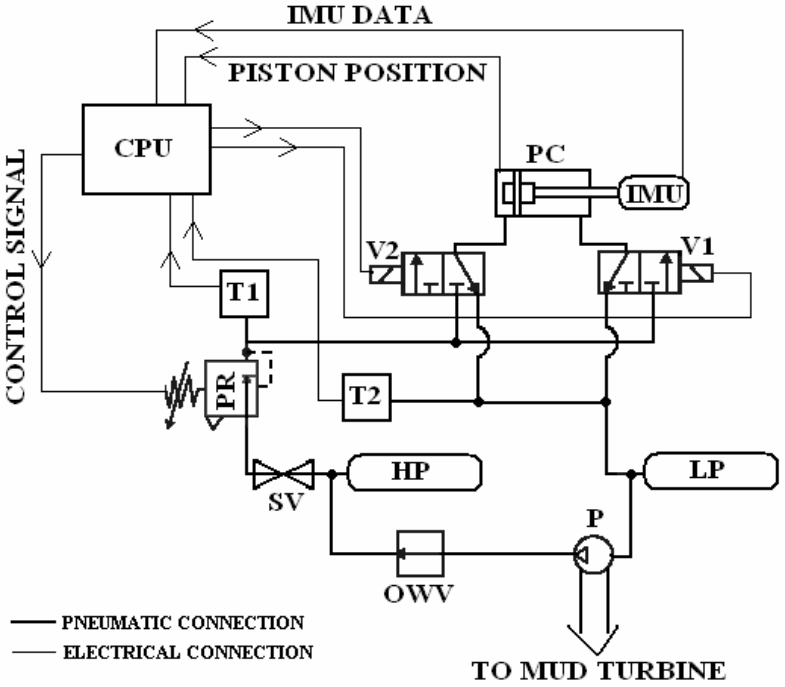

Fig.6: Pneumatic System Setup: HP-high pressure air tank; LP-low pressure air tank; PC-pneumatic cylinder, cushioned at both ends; V1, V2-two way solenoid valves; PR-proportional electric pressure regulator, T1, T2-electric pressure transducers, SV-shutoff valve; OWV-one-way air valve; P-air pump.

Initially, the system comprises a high (HP) and a low (LP) pressurized air tanks. The Central Processing Unit (CPU) can independently control the two solenoid valves (V1) and (V2) through which the pneumatic cylinder is connected to the rest of the pneumatic system. By feeding the appropriate signals to the two valves, the right chamber of the cylinder may be connected to the low-pressurized air tank, and the left to the highly-pressurized (HP) air tank via the electronic pressure regulator (PR). Then the two electric pressure transducers (T1) and (T2) inform the CPU of the air pressure in each chamber of the cylinder. Based on this information, the CPU calculates the necessary regulated pressure and controls the proportional regulator (PR). Once a pressure differential is established across the piston, a linear acceleration on the piston-IMU assembly is induced. A measurement of the piston's position is supplied to the CPU by the magnetostrictive effect-based measuring unit. The three acceleration components and angular rates measured by the IMU are also passed to the CPU where, together with the position of the piston, the data is processed mathematically to align the IMU.

Once the piston of the pneumatic cylinder is near the end of its stroke, the CPU reverses the valves (V1 and V2) and an opposite acceleration is induced. Cushions are provided on both sides of the piston to reduce the severity of the impact with the cylinder's walls.

Eventually, the pressures in the two air tanks will equalize, limiting the number of piston cycles and thus the number of alignment data points. To restart the system, the mud-powered air pump is turned on to pressurize the HP air tank to its initial high pressure. This in turn will bring the LP tank back to its original low pressure. Air is pumped from the LP tank to the HP tank through a special one-way air valve (OWV) that will prevent air from leaking back to the LP tank through the pump P. This resetting procedure is only possible when there is mud flow. Thus, it will be performed during the drilling process. The IDA process takes place when the bottom-hole assembly is at rest.

2.4 Data Manipulation and Transmission

Since the IMU is constantly in motion during the IDA process, wiring the IMU will be impractical and will result in constant stress applied to the wires. To eliminate such problems, RF link is proposed between the IMU and a local receiving module mounted on the exterior surface of the tube through which the IMU is accelerated. Thus, the three components of acceleration and angular rate measured by the IMU are sent to a local RF receiving module and then, together with the cylinder's piston position are wired to the CPU. There, the data is mathematically processed to determine the position of the BHA in the horizontal North-East frame. It is then send to the surface by the conventional method of mud pulse telemetry [3].

2.5 Mathematical Model of the Pneumatic System

To model the pneumatic system extensively, first a model of the pneumatic cylinder for its specific application will be derived. Throughout the entire model, all pneumatic processes are assumed to be adiabatic and the fluid (gas) is treated ideally. It has been shown that such assumptions still provide excellent results for similar applications, while greatly simplifying the model [10].

Let the cylinder be divided into two separate chambers A and B. Also, assume that the piston is moving to the right with speed v, (Fig.7).

The pressure change in chamber A is described by [10]:

$$\dot{P}_a = \left(\dot{m}_a - \frac{P_a A_a}{RT_s} \dot{x} \right) \frac{c_p R T_s}{c_v \left(V_{da} + \left(\frac{x_1}{2} + x \right) A_a \right)} \qquad (2)$$

where m_a and P_a are the mass of gas and pressure in chamber A respectively, and A_a is the area of the piston's surface enclosing chamber A.

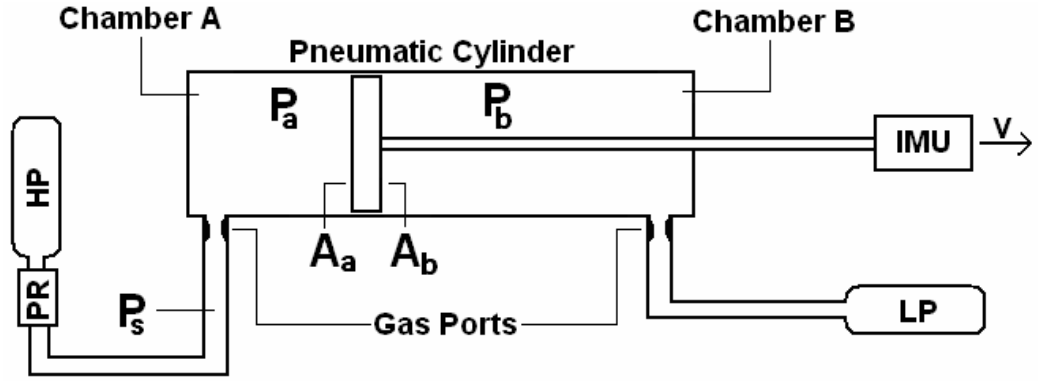

Fig.7: Supplying air to the cylinder: HP-high-pressure tank; LP-low pressure tank, PR-pressure regulator; P_a, P_b – pressure in chamber A and B respectively; P_s-supplied pressure by regulator (PR), A_a, A_b – area of piston common to chamber A and B respectively.

The position of the piston in the cylinder is denoted by x, while x_1 denotes the cylinder's stroke; Vda is the dead volume entitled to chamber A (tubing volume and unused cylinder volume). The temperature of the supplied gas is T_s, and c_p and c_v stand for the constant pressure and volume specific heats of the gas respectively; R is the gas constant. The rate of change of mass of gas in chamber A is given by [10]:

$$\dot{m}_a = \frac{c_q a P_s}{\sqrt{T_s}} \sqrt{\frac{2.8}{R(\gamma - 1)} \left[\left(\frac{P_a}{P_s} \right)^{\frac{2}{\gamma}} - \left(\frac{P_a}{P_s} \right)^{\frac{\gamma+1}{\gamma}} \right]} \quad (3)$$

In (3), c_q is the flow discharge coefficient of the pneumatic cylinder's inlet, a is the area of the inlet; and γ is the specific heat ratio. Similarly, the pressure change model for chamber B is [10]:

$$\dot{P}_b = \left(\dot{m}_b + \frac{P_b A_b}{R T_s} \dot{x} \right) \frac{c_p R T_s}{c_v \left(V_{db} + \left(\frac{x_1}{2} - x \right) A_b \right)} \quad (4)$$

where the variables correspond to the ones defined in Eq.(2), but applicable to chamber B. The rate of change of gas mass in chamber B is quantified similarly [10]:

$$\dot{m}_b = \frac{c_q a P_b}{\sqrt{T_b}} \sqrt{\frac{2.8}{R(\gamma - 1)} \left[\left(\frac{P_{ex}}{P_b} \right)^{\frac{2}{\gamma}} - \left(\frac{P_{ex}}{P_b} \right)^{\frac{\gamma+1}{\gamma}} \right]} \quad (5)$$

where, T_b is the temperature of chamber B, and P_{ex} is the exhaust pressure (pressure of LP tank).

Furthermore, the supplied pressure P_s that appears in Eq. (3) is the regulated pressure that comes from the proportional pressure regulator PR (Fig.6). However, since P_s is estimated by the CPU based only on the readings of the two pressure transducers T1 and T2 (Fig.6), it can be concluded that:

$$P_s = f(T_1, T_2) \quad (6)$$

Additionally, the motion of the IMU-piston assembly can be modeled by [10]:

$$M(\ddot{x} + g') + D\dot{x} = P_a A_a - P_b A_b + \hat{x} k \Delta \quad (7)$$

where M is the total mass of the IMU-containing capsule, piston and rod; x is the position of the piston inside the cylinder; D is some constant dependant on the materials used and the construction of the apparatus; g' is the component of Earth's acceleration parallel to the direction of induced motion on the IMU; k is the elasticity constant for the front and rear bumpers of the piston, and Δ is the change in length of the bumper. Equations 1-7 now completely define the pneumatic system for inducing a linear and angular motion on the IMU.

2.6 Materials

In order to implement the proposed design, the following materials and components were sourced.

- Pneumatic Cylinder (Cat. No. 2.00CJ2MABUS14AC20, Parker Pneumatics, Calgary, Alberta) with magnetostrictive linear position sensor (Cat. No. BTL5M1M0500RSU022KA02, Parker Pneumatics, Calgary, Alberta)
    - Cylinder Bore: 50.8mm
    - Cylinder Stroke: 508mm
    - Both sides cushioned magnetic piston:
        - Simulated Elasticity Constant(k): 20000N/m
        - Simulated Cushion Thickness: 5mm
    - Inlet/Outlet Air Ports
        - Flow Discharge Coefficient: 0.9
        - Port Cross-Section Area: $1.96*10^{-5}$ m^2
    - Dead Volumes
        - Chamber A/B : $1.96*10^{-3}$ m^3
- Electronic Proportional Pressure Regulator (Cat. No. PAR-15 W2154B179B, Parker Pneumatics, Calgary, Alberta)

- Analog Voltage Control (0-10V)
- Simulated Pressure Regulating Function:

```
Arguments (High pressure chamber (HP), Low pressure chamber (LP))
{
if ( HP-LP < 2000Pa AND LP+20kPa < pressure of high-pressure tank)
{
 Regulated Pressure = LP+20kPa
 }
else {Regulated Pressure = HP}
}
```

- Micro-electromechanical (MEM) Inertial Measurement Unit (MEMSense 2693D, Rapid City, SD)
  - Accelerometers (A50)
    - Dynamic Range: ±50g
    - Drift: 0.3g
  - Gyroscopes (-1200C050)
    - Dynamic Range: ±1200º/s
  - Magnetometers (not utilized in the proposed design)
    - Dynamic Rang: ±1.9G
    - Drift: 2700ppm/ ºC
  - Absolute Maximum Ratings:
    - Operation Temperature: -40 ºC to 85 ºC
    - Acceleration (Shock): 2000g for 0.5ms

3. Results

3.1 Motion of the Piston-IMU Assembly

According to the derived model of the pneumatic system and the outlined parameters of each component, a C++ simulation (Bloodshed Dev C++, Bloodshed Software, www.bloodshed.net/devcpp.html) revealed the position of the piston in the pneumatic cylinder as a function of time (Fig.8).

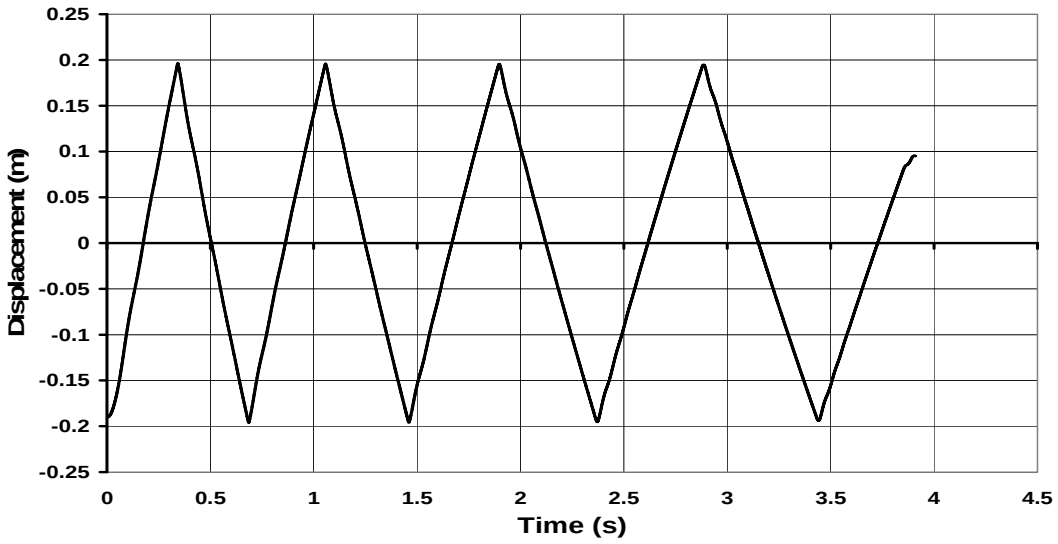

Fig.8: The displacement of the piston inside the pneumatic cylinder as a function of time. The displacement is with respect to the middle of the stroke of the cylinder.

Figure 8 demonstrates that a tank, initially pressurized to ten atmospheres will allow the completion of four full cycles in less than 3.5 seconds. The piston can be then brought to rest during the fifth cycle and locked in place by completely closing the inlet and outlet ports of the cylinder. The acceleration of the piston-IMU assembly was also simulated over the duration of a full cycle (Fig.9).

The constantly changing acceleration of the piston (Fig.9) is due to the specifically implemented function in the simulation, relating the two electronic pressure transducer outputs to the regulated pressure adjusted by the proportional pressure regulator. For a sampling rate of 400Hz, the time intervals of 0 to 0.3 seconds and 0.35 to 0.6 seconds will be proper choices for observations source. The data obtained in these time intervals can then be utilized in aligning the IMU sensors. However, a more gradually changing acceleration of the piston is desired in order to align the IMU more accurately.

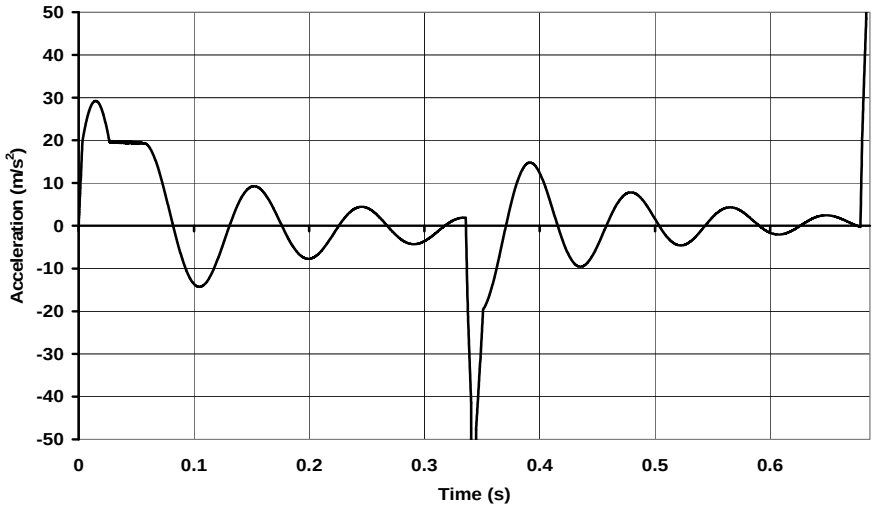

Fig.9: Piston's acceleration as a function of time during one full cycle. The acceleration peaks at 0.34s and 0.68s correspond to the accelerations experienced by the IMU-piston assembly when the piston's bumper collides with the cylinder's wall.

The pressure in each tank as a function of time during the entire induced motion process has also been explored (Fig.10).

It is clearly evident that after 3.8s (for the outlined system parameters), the pressures in the two tanks will equalize, and the induced motion will come to an end. At this point, the mud-powered air pump is turned on to pressurize the high-pressure tank to its initial value. Although the currently implemented pressure regulating function will yield economical use of the fluid (air), a function that will provide more gradual accelerations of the piston is desired.

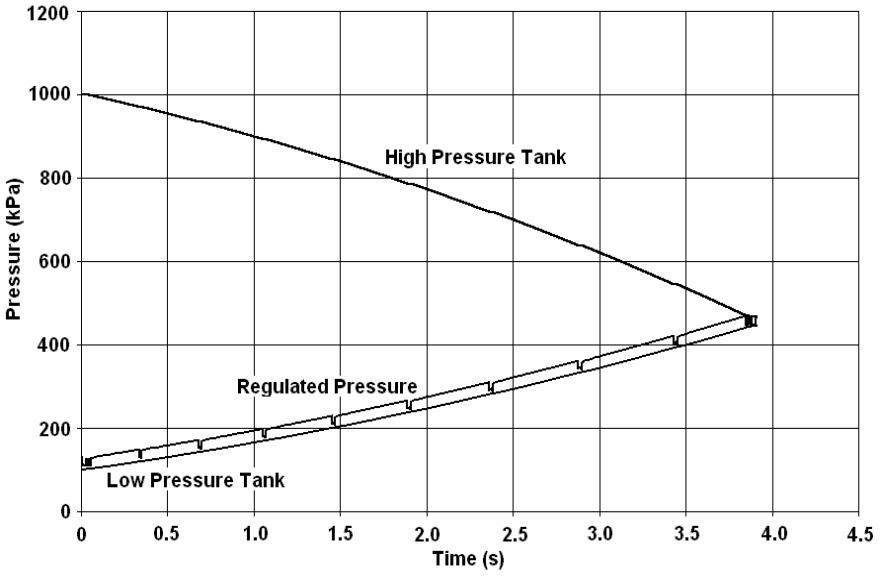

Fig.10: Output of the proportional pressure regulator, and pressures of the high and low-pressure tanks as a function of time over the entire induced motion process.

4. Conclusion

This article focused on designing and quantifying an apparatus that will allow for an effective, simple and low cost aligning of the sensors of an Inertial-Measurement Unit for continuous angle attitude angle information delivery in a downhole drilling environment. A pneumatic solution was proposed, comprising an air-cylinder, two air tanks, air-pump and a proportional pressure regulator. The highly pressurized air-tank is discharged into the low-pressure tank through the air-cylinder. Correct control of the pressure on each side of the piston of the air-cylinder yields the desired accelerations of the IMU-piston assembly. The position of the piston is constantly monitored by a magnetostrictive sensor, which in turn is differentiated to give the acceleration of the IMU-piston assembly. Moreover, by moving the IMU along a helical thread, angular motion is induced on it, whose angular acceleration is a simple function of the linear acceleration. Once the IMU's angular and linear motion components are known, they are utilized in aligning the unit.

A mathematical model of the entire pneumatic system was derived and simulated with C++. It was shown that an air tank with initial pressure of ten atmospheres will yield more than four full alignment cycles of the IMU-piston assembly within a timeframe of four seconds. The induced accelerations on the IMU-piston assembly were in the range of 3g's, except during a collision with the walls of the air-cylinder, where they reach 80g's. Despite the fact that the model showed a feasible design in downhole conditions, a pressure regulating function that will allow more gradual induced accelerations is desired.

Bibliography

[1] J. Burkmann and N. Nickels, "Directional, navigational and horizontal drilling techniques," *Geothermal Resources Council Bull*., vol. V19, no.4, pp. 106-112, 1990.

[2] S.D. Joshi and W. Ding, "The cost benefits of horizontal drilling," In *Proc. American Gas Association*, Arlington, VA, Apr.-May 29-1, 1991, pp.679-684.

[3] S. D. Joshi, "Horizontal Well Technology", *Technology and Industrial Arts*, PennWell Books, 1991

[4] E.K. Fisher and M.R. French, "Drilling the first horizontal well in the Gulf of Mexico: A case history of East Cameron block 278 well B-12," in *Proc. 66th SPE Annu. Technical Conf. Exhibition*, Dallas, TX, Oct.6-9, 1991, pp.111-123

[5] C. Walker, "Drill Bit Steering," US. Patent 5311953, May 17, 1994

[6] B.A. Shelkholeslami, B.W. Schlottman, F.A. Siedel, and D.M. Button, "Drilling and production aspects of horizontal wells in the Austin Chalkl," *J. Petroleum Technol*., pp.773-779, Jul.1991.

[7] A. Noureldin, "New measurement-while drilling surveying technique utilizing a set of fiber-optic rotation sensors," Ph.D. Dissertation, Dept. Elect. Eng., Univ. Calgary, Calgary, AB, Canada, 2002.

[8] A. Noureldin, D. Irvine-Halliday, and M.P. Mintchev, "Accuracy Limitations of FOG-Based Continuous Measurement-While-Drilling Surveying Instruments for Horizontal Wells," *IEEE Trans. On Instr. And Meas.*, vol.51, no.6, Oct. 2002.

[9] E. Pecht, "INS In-Drilling Alignment for improving Observability in Horizontal-Directional Drilling,"Ph.D. Dissertation, Dept. Elect. Eng., Univ. Calgary, Calgary, AB, Canada, 2005.

[10] R. Richardson, A.R. Plummer, M. Brown, "Modeling and simulation of pneumatic cylinders for a physiotherapy robot," School of Mech. Eng., University of Leeds, UK,

[11] O. Sound, "Linear Position Sensor Option for Series 2MA Cylinder," Parker Hannifin Corporation, Des Plaines, IL USA

[12] P. Tubel, C. Bergeron, S. Bell, "Mud pulse telemetry system for downhole measurement-while-drilling," *IEEE Instr. And Meas. Tech. Conf.*, 1992, p 219-23

[13] J.L. Thorogood and D. R. Knott, "Surveying techniques with a solid state magnetic multi-shot device," in *Proc. SPE/IADC Drilling Conf*., New Orleans, LA, Feb. 28-March 3, 1989, pp.841-856.

Authors' Information

Alexander Djurkov – Department of Electrical and Computer Engineering, University of Calgary, Alberta, Canada, T2N 1N4. Phone: (403) 244-2298; e-mail: alexsd_bg@yahoo.co.uk

Justin Cloutier – Imperial Oil Ltd., Calgary, Alberta, Canada; Department of Electrical and Computer Engineering, University of Calgary, Alberta, Canada, T2N 1N4; Phone: (403) 220-2191.

Martin P. Mintchev – Prof., Dr., Department of Electrical and Computer Engineering; University of Calgary; Calgary, Alberta, Canada, T2N 1N4; Department of Surgery, University of Alberta; Edmonton, Alberta T6G 2B7; Phone: (403) 220-5309; Fax (403) 282-6855; e-mail: mintchev@ucalgary.ca